JHEP

Published for SISSA by Springer

Received: February 26, 2015
Accepted: May 8, 2015
Published: May 25, 2015

Inverse magnetic catalysis in holographic models of QCD

Kiminad A. Mamo

Department of Physics, University of Illinois, Chicago, IL 60607, U.S.A.

E-mail: kabebe2@uic.edu

Abstract: We study the effect of magnetic field B on the critical temperature T_c of the confinement-deconfinement phase transition in hard-wall AdS/QCD, and holographic duals of flavored and unflavored $\mathcal{N} = 4$ super-Yang Mills theories on $\mathbb{R}^3 \times \mathrm{S}^1$. For all of the holographic models, we find that $T_c(B)$ decreases with increasing magnetic field $B \ll T^2$, consistent with the *inverse magnetic catalysis* recently observed in lattice QCD for $B \lesssim 1\,\mathrm{GeV}^2$. We also predict that, for large magnetic field $B \gg T^2$, the critical temperature $T_c(B)$, eventually, starts to increase with increasing magnetic field $B \gg T^2$ and asymptotes to a constant value.

Keywords: Gauge-gravity correspondence, AdS-CFT Correspondence, Holography and quark-gluon plasmas

ArXiv ePrint: 1501.03262

doi:10.1007/JHEP05(2015)121

JHEP05(2015)121

Contents

JHEP05(2015)121

1 Introduction

Recently, the study of the QCD phase diagram for magnetic field B has attracted considerable attention [1–19], see [20] for a review. The main motivation for studying the QCD phase diagram under external magnetic field B stems from the fact that strong magnetic field B is produced in heavy ion collisions experiments at RHIC $eB \sim 0.01\,\mathrm{GeV}^2$ and LHC $eB \sim 0.25\,\mathrm{GeV}^2$ [21], due to the charged spectator particles, which has interesting effects on the quark-gluon plasma created during these heavy ion collision experiments [22–27], see [20] for a review. A strong magnetic field $eB \sim 4\,\mathrm{GeV}^2$ is also produced during the electroweak phase transition of the early Universe [28], and relatively weaker magnetic field $eB \sim 1\,\mathrm{MeV}^2$ is produced in the interior of dense neutron stars [29].

Another motivation comes from the fact that the study of the QCD phase diagram with magnetic field B is amenable to numerical simulations of QCD on the lattice, without

facing the sign problem of lattice QCD that exist in the case of non-zero baryon chemical potential μ_B, creating an opportunity to compare the holographic and low energy effective models of QCD directly with QCD itself.

Regarding the study of the QCD phase diagram for magnetic field B, most of the models for QCD [1–10], including the holographic ones [11–16], have studied chiral-symmetry-restoration transition and have predicted that the critical temperature T_c of the transition increases with increasing magnetic field B at zero chemical potential $\mu = 0$. This enhancing effect of the magnetic field B on the critical temperature T_c has been termed *magnetic catalysis*. However, recent lattice QCD result [19] has indicated the opposite effect, that is, the critical temperature T_c decreases with increasing magnetic field B, for $B \lesssim 1\,\mathrm{GeV}^2$ and zero chemical potential $\mu = 0$. This inhibiting effect of the magnetic field B on the critical temperature T_c has been termed *inverse magnetic catalysis*.

Even though, the recent lattice QCD result [19] has also indicated that the confinement-deconfinement and chiral symmetry breaking phase transitions occur at the same critical temperature $T_c(B)$ at least for $B \lesssim 1\,\mathrm{GeV}^2$, most holographic calculations so far [11–17] have been concerned only with $T_c(B)$ of the chiral symmetry breaking phase transition. However, recently, reference [18], inspired by the recent lattice QCD result [19], has a priori assumed confinement and chiral symmetry breaking transitions to occur at the same critical temperature T_c in Sakai-Sugimoto model, and has argued that, in this case, $T_c(B)$ must be a decreasing function of B, consistent with the recent lattice QCD result [19], but has not provided a direct computation of $T_c(B)$.

In this paper, we give a direct computation of the critical temperature $T_c(B)$ of the confinement-deconfinement phase transition in hard-wall AdS/QCD, and holographic duals of flavored and unflavored $\mathcal{N} = 4$ SYM on $\mathbb{R}^3 \times \mathrm{S}^1$ where S^1 is a circle of length l in one of the spatial directions. (Note that, at finite temperature T, $\mathbb{R}^3$ is really $S^1_\tau \times \mathbb{R}^2$ where S^1_τ is the thermal circle with length $\frac{1}{T}$.) Also, note that, since the fermions of both the flavored and unflavored $\mathcal{N} = 4$ SYM on $\mathbb{R}^3 \times \mathrm{S}^1$ obey antiperiodic boundary conditions around the circle S^1, they acquire a tree-level mass $m \sim \frac{1}{l}$. The scalars are periodic around the circle, hence they acquire masses only at the quantum level through their couplings to the fermions [34]. The gluons, however, do not acquire masses, therefore, at low-energy, both flavored and unflavored $\mathcal{N} = 4$ SYM on $\mathbb{R}^3 \times \mathrm{S}^1$ reduce to pure 3D Yang-Mills theory.

It is well known that both flavored and unflavored $\mathcal{N} = 4$ super-Yang Mills theories (SYM) on flat spacetime $\mathbb{R}^4$ are not confining gauge theories. However, they can be made confining in the large-N_c limit by placing them on a compact space with length l, and the confinement-deconfinement phase transition occurs at critical temperature $T_c = \frac{1}{l}$ [30, 31, 33], see [34, 35] for a review. In our case, the compact space is $\mathbb{R}^3 \times \mathrm{S}^1$, that is, we compactify one of the spatial dimensions into a circle of length l.

The confinement-deconfinement phase transition both in flavored and unflavored $\mathcal{N} = 4$ SYM on $\mathbb{R}^3 \times \mathrm{S}^1$ is holographically modeled by a phase transition between a black hole solution with radius of horizon $r = r_h$, and AdS_5-soliton solution which smoothly ends at $r = r_0$. However, to study the confinement-deconfinement phase transition in QCD on $\mathbb{R}^4$ at strong coupling, we use the hard-wall AdS/QCD model where the confinement-deconfinement phase transition, of QCD on $\mathbb{R}^4$, is holographically modeled by a phase

JHEP05(2015)121

transition between a black hole solution with radius of horizon $r = r_h$, and thermal-AdS_5 solution with hard-wall IR cut-off $r = r_0$.

We derive the corresponding thermal-AdS_5 solution which is the holographic dual to the confined phase of QCD on $\mathbb{R}^4$ by starting from a black hole solution, which corresponds to the deconfined phase of strongly coupled QCD on $\mathbb{R}^4$, by setting the mass of the black hole to zero [47]. And, we derive the corresponding AdS_5-soliton solution, which is the holographic dual to the confined phase of flavored and unflavored $\mathcal{N} = 4$ SYM on $\mathbb{R}^3 \times S^1$, by "double Wick rotating" a black hole solution [34, 35].

In this paper, we use two black hole solutions in the presence of constant magnetic field B. First, we use the black hole solution in the presence of constant magnetic field $B \ll T^2$ found in [36] to study the confinement-deconfinement phase transition in strongly coupled QCD on $\mathbb{R}^4$ and unflavored $\mathcal{N} = 4$ SYM on $\mathbb{R}^3 \times S^1$. Then, we use the black hole solution in the presence of constant magnetic field B, including the backreaction of N_f flavor or D7-branes for $N_f \ll N_c$, found in [38] to study the confinement-deconfinement phase transition in flavored $\mathcal{N} = 4$ SYM on $\mathbb{R}^3 \times S^1$.

The effect of magnetic field B on different observables has also been studied in [39–43] using the backreacted black hole solution of [36] without flavor D7-branes.

Depending on the specific holographic models to QCD, various length and energy scales appear throughout this paper. Some of the relevant length and energy scales are: the radius of the AdS_5 spacetime L which we set to $L = 1$, the radius of the black hole horizon r_h which is related to the Hawking temperature T_H of the black hole (which is dual to the field theory temperature $T = T_H$), the radial position of the canonical singularity of the AdS_5-soliton $r_0 = \pi T_c(B = 0) = \pi \times 0.175\,\text{GeV} = 0.55\,\text{GeV}$ for flavored and unflavored $\mathcal{N} = 4$ SYM on $\mathbb{R}^3 \times S^1$, the radial position of the hard-wall $r_0 = \frac{m_\rho}{2.405} = 0.323\,\text{GeV}$ in the thermal-AdS_5 solution for the hard-wall AdS/QCD, and an external magnetic field B in the range of $0 - 0.35\,\text{GeV}^2$ for the hard-wall AdS/QCD model and $0 - 4.2\,\text{GeV}^2$ for the flavored $\mathcal{N} = 4$ SYM on $\mathbb{R}^3 \times S^1$.

The outline of this paper is as follows: in section 2, we write down the 5-dimensional Einstein-Maxwell action (which will be used to study confinement-deconfinement phase transition in hard-wall AdS/QCD and holographic dual of unflavored $\mathcal{N} = 4$ SYM on $\mathbb{R}^3 \times S^1$) including the Gibbons-Hawking surface term and the appropriate counter terms. We then review the black hole solution in the presence of constant magnetic field $B \ll T^2$ found in [36]. Then, starting from the black hole solution, which corresponds to the deconfined phase of strongly coupled QCD on flat spacetime and unflavored $\mathcal{N} = 4$ SYM on $\mathbb{R}^3 \times S^1$, we derive the corresponding thermal-AdS_5 and AdS_5-soliton solutions, which correspond to the confined phases of strongly coupled QCD on flat spacetime and unflavored $\mathcal{N} = 4$ SYM on $\mathbb{R}^3 \times S^1$, respectively. We also determine the on-shell Euclidean actions (free energies) for the black hole, thermal-AdS_5, and AdS_5-soliton solutions.

In section 3, we compute the critical temperature T_c of the confinement-deconfinement phase transition in hard-wall AdS/QCD, and holographic duals of flavored and unflavored $\mathcal{N} = 4$ SYM on $\mathbb{R}^3 \times S^1$. We first compute the critical temperature T_c of the confinement-deconfinement phase transition in hard-wall AdS/QCD by requiring the difference between the black hole and thermal-AdS_5 on-shell Euclidean actions vanish at $T = T_c$. Then, we

JHEP05(2015)121

compute the critical temperature T_c of the confinement-deconfinement phase transition in holographic dual of unflavored $\mathcal{N}=4$ SYM on $\mathbb{R}^3\times \mathrm{S}^1$ by requiring the difference between the black hole and AdS_5-soliton on-shell Euclidean actions vanish at $T=T_c$. Finally, using the insight we gained, in computing the critical temperature T_c of the confinement-deconfinement phase transition in holographic dual of unflavored $\mathcal{N}=4$ SYM on $\mathbb{R}^3\times \mathrm{S}^1$, we compute the critical temperature T_c of the confinement-deconfinement phase transition in holographic dual of flavored $\mathcal{N}=4$ SYM on $\mathbb{R}^3\times \mathrm{S}^1$ by constructing the backreacted AdS_5-soliton solution from the backreacted black hole metric of D3/D7 model, with magnetic field B, found in [38].

In appendix A, we compute the critical temperature $T_c(B)$ of the confinement-deconfinement phase transition in hard-wall AdS/QCD for large magnetic field $B\gg T^2$.

2 Einstein-Maxwell theory in 5D

In this section, we review elements of Einstein-Maxwell theory in 5D which will, subsequently, be used to study confinement-deconfinement phase transitions in hard-wall AdS/QCD and holographic dual of unflavored $\mathcal{N}=4$ SYM on $\mathbb{R}^3\times \mathrm{S}^1$.

The action of five-dimensional Einstein-Maxwell theory with a negative cosmological constant is [36][1]

$$S=S_{\text{bulk}}+S_{\text{bndy}}\,, \tag{2.1}$$

where the bulk action S_{bulk} is

$$S_{\text{bulk}}=\frac{1}{16\pi G_5}\int d^5x\sqrt{-g}\left(R-F^{MN}F_{MN}+\frac{12}{L^2}\right), \tag{2.2}$$

and the boundary action S_{bndy} is

$$S_{\text{bndy}}=\frac{1}{8\pi G_5}\int d^4x\sqrt{-\gamma}\left(K-\frac{3}{L}+\frac{L}{2}\left(\ln\frac{r}{L}\right)F^{\mu\nu}F_{\mu\nu}\right)\Big|_{r=r_\Lambda}. \tag{2.3}$$

In the boundary action S_{bndy} (2.3), the first term is the Gibbons-Hawking surface term, and the other terms are the counter terms needed to cancel the $\mathrm{UV}(r_\Lambda\to\infty)$ divergences in the bulk action in accordance with the holographic renormalization procedure [46]. Note that the counter terms are entirely constructed from the induced metric $\gamma_{\mu\nu}$ on the boundary surface at $r=r_\Lambda$, that is,

$$\gamma_{\mu\nu}(r_\Lambda)=\mathrm{diag}\left(g_{tt}(r_\Lambda),g_{xx}(r_\Lambda),g_{yy}(r_\Lambda),g_{zz}(r_\Lambda)\right). \tag{2.4}$$

And, K is the trace, with respect to $\gamma_{\mu\nu}$, of the extrinsic curvature of the boundary given by $K_{\mu\nu}=(\partial_r\gamma_{\mu\nu})/(2\sqrt{g_{rr}})$. Using the matrix formula $\partial_\mu(\det M)=\det M\,\mathrm{tr}(M^{-1}\partial_\mu M)$ [35], we can write $K=\gamma^{\mu\nu}K_{\mu\nu}=\frac{\sqrt{g^{rr}}\partial_r\sqrt{\gamma}}{\sqrt{\gamma}}$ [35, 36].

[1] Our conventions here are such that the Ricci scalar here R_{here} is related to the Ricci scalar there R_{there} (given in [36]) by $R_{\text{here}}=-R_{\text{there}}$.

JHEP05(2015)121

In addition to the Bianchi identity, the field equations are [36]

$$R_{MN} = -\frac{4}{L^2}g_{MN} - \frac{1}{3}F^{PQ}F_{PQ}g_{MN} + 2F_{MP}F_N{}^P\,, \tag{2.5}$$

$$\nabla^M F_{MN} = 0\,. \tag{2.6}$$

From now on we set the AdS radius to unity, that is, $L = 1$.

Turning on a constant bulk magnetic field, in the z-direction, $B_z = F_{xy} = \partial_x A_y - \partial_y A_x = B$, where the bulk gauge potential $A_\mu(x,r) = \frac{1}{2}B(x\delta^y_\mu - y\delta^x_\mu)$,[2] which solves Maxwell's equation (2.6), and contracting Einstein's field equation (2.5), one can find the Ricci scalar $R = g^{MN}R_{MN}$ to be

$$R = -20 + \frac{2}{3}B^2 g^{xx}g^{yy}. \tag{2.7}$$

So, the on-shell Euclidean action $S_{\rm E}$ (which can be found from the Lorentzian action (2.1) by analytic continuation in the imaginary time direction, i.e., $t_E = it$) takes the form

$$S_{\rm E} = S^{\rm E}_{\rm bulk} + S^{\rm E}_{\rm bndy}\,, \tag{2.8}$$

where the on-shell Euclidean bulk action $S^{\rm E}_{\rm bulk}$ is

$$S^{\rm E}_{\rm bulk} = \frac{V_3}{8\pi G_5}\int_0^\beta dt_E \int_{r'}^{r_\Lambda} dr\sqrt{g}\left(4 + \frac{2}{3}B^2 g^{xx}g^{yy}\right), \tag{2.9}$$

and, the on-shell Euclidean boundary action $S^{\rm E}_{\rm bndy}$ is

$$S^{\rm E}_{\rm bndy} = -\frac{V_3}{8\pi G_5}\int_0^\beta dt_E \sqrt{\gamma}\left(K - 3 + B^2 g^{xx}g^{yy}\ln r_\Lambda\right), \tag{2.10}$$

and, r_Λ is the UV cut-off while r' is the radius of the horizon $r' = r_h$ for a black hole solution, and IR cut-off $r' = r_0$ for a thermal-AdS$_5$ or AdS$_5$-soliton solutions. From now on we set $V_3 = 8\pi G_5 = 1$. Also, note that the on-shell Euclidean action $S_{\rm E}$ is related to the free energy F by $S_{\rm E} = \beta F$.

2.1 Background solutions with $B \ll T^2$

In this subsection, we review the black hole solution in the presence of constant magnetic field $B \ll T^2$ found in [36] which corresponds to the deconfined phase of strongly coupled QCD on $\mathbb{R}^4$ (flat spacetime) and unflavored $\mathcal{N} = 4$ SYM on $\mathbb{R}^3 \times \mathrm{S}^1$. Then, starting from the black hole solution, by setting the mass of the black hole to zero [47], we derive the corresponding thermal-AdS$_5$ solution which is the holographic dual to the confined phase of strongly coupled QCD on flat spacetime $\mathbb{R}^4$. And, by "double Wick rotating" the black hole solution [34, 35], we derive the corresponding AdS$_5$-soliton solution which is the holographic dual to the confined phase of unflavored and strongly coupled $\mathcal{N} = 4$ SYM on $\mathbb{R}^3 \times \mathrm{S}^1$.

[2] Note that the bulk gauge potential $A_\mu(x,r)$ and the corresponding bulk magnetic field $B = F_{xy}(x,r)$ are dual to the boundary gauge potential $A_\mu(x) = A_\mu(x, r=\infty)$ and the corresponding boundary magnetic field $B = F_{xy}(x, r=\infty)$ which couple to the U(1) charged particles of the field theory living at the boundary. Later on, when we start discussing specific holographic models to QCD, we will specify the type of global U(1) gauge group and the associated boundary current $J^\mu(x)$.

JHEP05(2015)121

2.1.1 Black hole

For $B \ll T^2$ and electric charge density ρ, the perturbative black hole solution in powers of B, up to an integration constant a_3 is given in eq. 6.1 and 6.16 of ref. [36]. Here, we set the electric charge density $\rho = 0$ and fix the integration constant $a_3 = -\frac{2}{3}$ so that the perturbative solution in powers of B matches the near boundary solution which is also given in eq. 4.4, 4.5 and 6.16 of [36]. Therefore, the black hole solution in eq. 6.1 and 6.16 of ref. [36], for vanishing electric charge density $\rho = 0$ and $a_3 = -\frac{2}{3}$, takes the form

$$\begin{aligned} ds^2_{\text{bh}} &= r^2\left(-f(r)dt^2 + q(r)dz^2 + h(r)\left(dx^2+dy^2\right)\right) + \frac{dr^2}{f(r)r^2}\,, \\ f(r) &= 1 - \frac{M}{r^4} - \frac{2}{3}B^2\frac{\ln r}{r^4} + \mathcal{O}(B^4)\,, \\ q(r) &= 1 - \frac{2}{3}B^2\frac{\ln r}{r^4} + \mathcal{O}(B^4)\,, \\ h(r) &= 1 + \frac{1}{3}B^2\frac{\ln r}{r^4} + \mathcal{O}(B^4)\,, \end{aligned} \tag{2.11}$$

and, the Hawking temperature T becomes

$$T = \frac{1}{\beta} = U'(r_h) = \frac{r_h}{2\pi}\left(1 + \frac{M}{r_h^4} - \frac{2}{3}B^2\left(\frac{1}{2r_h^4} - \frac{\ln r_h}{r_h^4}\right)\right) + \mathcal{O}(B^4)\,, \tag{2.12}$$

where M is the mass of the black hole, $U(r) = r^2 f(r)$, the radius of the horizon r_h is defined by requiring $f(r = r_h) = 0$, T is the Hawking temperature of the black hole, and β is the length of the thermal circle which acquired a fixed value as a function of r_h in order to avoid the canonical singularity at the horizon $r = r_h$. One can also check that (2.11) indeed satisfies the Einstein field equation (2.5) or its contracted version (2.7).

2.1.2 Thermal-AdS$_5$

The thermal-AdS$_5$ solution can be found from a black hole solution by setting the mass of the black hole M to zero, see [47] for the electrically charged black hole case. Therefore, from the black hole solution for $B \ll T^2$ (2.11), we can determine the thermal-AdS solution for $B \ll \Lambda_{IR}^2 \sim r_0^2$ by setting the mass of the black hole $M = 0$,

$$\begin{aligned} ds^2_{\text{thermal}} &= r^2\left(-f_0(r)dt^2 + q(r)dz^2 + h(r)\left(dx^2+dy^2\right)\right) + \frac{dr^2}{f_0(r)r^2}\,, \\ f_0(r) &= 1 - \frac{2}{3}B^2\frac{\ln r}{r^4} + \mathcal{O}(B^4)\,, \\ q(r) &= 1 - \frac{2}{3}B^2\frac{\ln r}{r^4} + \mathcal{O}(B^4)\,, \\ h(r) &= 1 + \frac{1}{3}B^2\frac{\ln r}{r^4} + \mathcal{O}(B^4)\,. \end{aligned} \tag{2.13}$$

2.1.3 AdS$_5$-soliton

The AdS$_5$-soliton solution [32, 33] can be determined from the black hole solution (2.11) by "double Wick rotation" $t = iz'$ and $z = it'$ [34, 35]. Therefore, for $B \ll \Lambda_{IR}^2 \sim r_0^2$ the

JHEP05(2015)121

AdS_5-soliton solution is,

$$
\begin{aligned}
ds^2_{\text{soliton}} &= r^2\left(f_s(r)dz'^2 - q(r)dt'^2 + h(r)\left(dx^2+dy^2\right)\right) + \frac{dr^2}{f_s(r)r^2}\,, \qquad (2.14)\\
f_s(r) &= 1 - \frac{M}{r^4} - \frac{2}{3}B^2\frac{\ln r}{r^4} + \mathcal{O}(B^4)\,,\\
q(r) &= 1 - \frac{2}{3}B^2\frac{\ln r}{r^4} + \mathcal{O}(B^4)\,,\\
h(r) &= 1 + \frac{1}{3}B^2\frac{\ln r}{r^4} + \mathcal{O}(B^4)\,,\\
\frac{1}{l} &= \frac{U'(r_0)}{4\pi} = \frac{r_0}{2\pi}\left(1 + \frac{M}{r_0^4} + \frac{2}{3}B^2\left(\frac{\ln r_0}{r_0^4} - \frac{1}{2r_0^4}\right)\right) + \mathcal{O}(B^4).
\end{aligned}
$$

where l is the length of the circle in the compactified z' direction which is arbitrary for the black hole solution but in order to avoid the canonical singularity at $r = r_0$ (where r_0 is defined by requiring $f_s(r = r_0) = 0$), it acquires a finite value which is given in terms of r_0 for the AdS_5-soliton solution (2.14).

2.2 On-shell Euclidean actions with $B \ll T^2$

In this subsection, we determine the on-shell Euclidean actions (free energies) for the black hole, thermal-AdS_5, and AdS_5-soliton solutions. And, we compute the difference between the on-shell Euclidean actions of the deconfining geometry (which is the black hole geometry for both hard-wall AdS/QCD and holographic dual of unflavored $\mathcal{N} = 4$ SYM on $\mathbb{R}^3 \times S^1$) and the confining geometry (which is the thermal-AdS_5 geometry for hard-wall AdS/QCD, and the AdS_5-soliton geometry for holographic dual of unflavored $\mathcal{N} = 4$ SYM on $\mathbb{R}^3 \times S^1$).

2.2.1 Black hole

The on-shell Euclidean action $S_{\text{E}} = S_{\text{bh}}$ (2.8) for the black hole solution with $B \ll T^2$ (2.11) is

$$S_{\text{bh}} = S_{\text{bulk}} + S_{\text{bndy}}, \qquad (2.15)$$

where the on-shell Euclidean bulk action of the black hole S_{bulk} for $B \ll T^2$ is

$$S_{\text{bulk}} = \int_0^\beta dt_E \int_{r_h}^{r_\Lambda} dr\sqrt{g}\left(4 + \frac{2}{3}B^2 g^{xx}g^{yy}\right), \qquad (2.16)$$

and the on-shell Euclidean boundary action of the black hole S_{bndy} for $B \ll T^2$ is

$$S_{\text{bndy}} = -\int_0^\beta dt_E\sqrt{\gamma}\left(\frac{\sqrt{g^{rr}}\partial_r\sqrt{\gamma}}{\sqrt{\gamma}} - 3 + B^2 g^{xx}g^{yy}\ln r_\Lambda\right). \qquad (2.17)$$

The bulk action S_{bulk} (2.16) (after using the black hole metric for $B \ll T^2$ (2.11), using the fact that $h(r)\sqrt{q(r)} = 1 + \mathcal{O}(B^4)$, evaluating the integrals, and simplifying) become

$$S_{\text{bulk}} = -\beta\left(r_h^4 - r_\Lambda^4 - \frac{2}{3}B^2\ln r_\Lambda + \frac{2}{3}B^2\ln r_h\right) + \mathcal{O}(B^4), \qquad (2.18)$$

JHEP05(2015)121

which diverges when $r_\Lambda \to \infty$, and the boundary action $S_{\rm bndy}$ (2.17) becomes

$$S_{\rm bndy} = -\beta\left(r_\Lambda^4 + \frac{2}{3}B^2 \ln r_\Lambda - \frac{1}{2}M - \frac{1}{3}B^2\right) + \mathcal{O}(B^4), \tag{2.19}$$

where we ignored terms which goes to zero in the $r_\Lambda \to \infty$ limit. Also note that (2.19) diverges when $r_\Lambda \to \infty$, but the sum of $S_{\rm bulk}$ (2.18) and $S_{\rm bndy}$ (2.19) is finite. Hence, the black hole on-shell Euclidean action $S_{\rm bh}$ (2.15) is

$$S_{\rm bh} = S_{\rm bulk} + S_{\rm bndy} = -\beta\left(r_h^4 - \frac{1}{2}M + \frac{2}{3}B^2 \ln r_h - \frac{1}{3}B^2\right) + \mathcal{O}(B^4)\ . \tag{2.20}$$

2.2.2 Thermal-AdS$_5$

The on-shell Euclidean action $S_{\rm E} = S_{\rm thermal}$ (2.8) for the thermal-AdS$_5$ solution with $B \ll \Lambda_{IR}^2 \sim r_0^2$ (2.13) is

$$S_{\rm thermal} = S_{\rm tbulk} + S_{\rm tbndy}, \tag{2.21}$$

where the on-shell Euclidean bulk action $S_{\rm tbulk}$ of the thermal-AdS$_5$ for $B \ll \Lambda_{IR}^2 \sim r_0^2$ is

$$S_{\rm tbulk} = \int_0^{\beta'} dt_E \int_{r_0}^{r_\Lambda} dr \sqrt{g}\left(4 + \frac{2}{3}B^2 g^{xx} g^{yy}\right), \tag{2.22}$$

and the on-shell Euclidean boundary action $S_{\rm tbndy}$ of the thermal-AdS$_5$ for $B \ll T^2$ is

$$S_{\rm tbndy} = -\int_0^{\beta'} dt_E \sqrt{\gamma}\left(\frac{\sqrt{g^{rr}}\partial_r\sqrt{\gamma}}{\sqrt{\gamma}} - 3 + B^2 g^{xx} g^{yy} \ln r_\Lambda\right). \tag{2.23}$$

The thermal-AdS$_5$ bulk action $S_{\rm tbulk}$ (2.22) (after using the thermal-AdS$_5$ metric for $B \ll T^2$ (2.13), using the fact that $h(r)\sqrt{q(r)} = 1 + \mathcal{O}(B^4)$, evaluating the integrals, and simplifying) becomes

$$S_{\rm tbulk} = -\beta'\left(r_0^4 - r_\Lambda^4 - \frac{2}{3}B^2 \ln r_\Lambda + \frac{2}{3}B^2 \ln r_0\right) + \mathcal{O}(B^4), \tag{2.24}$$

which diverges when $r_\Lambda \to \infty$, and the thermal-AdS$_5$ boundary action $S_{\rm tbndy}$ (2.23) becomes

$$S_{\rm tbndy} = -\beta'\left(r_\Lambda^4 + \frac{2}{3}B^2 \ln r_\Lambda - \frac{1}{3}B^2\right) + \mathcal{O}(B^4), \tag{2.25}$$

which diverges as well when $r_\Lambda \to \infty$. But, the sum of $S_{\rm tbulk}$ (2.24) and $S_{\rm tbndy}$ (2.25) is finite. Hence, the thermal on-shell Euclidean action $S_{\rm thermal}$ (2.21) becomes

$$S_{\rm thermal} = -\beta\left(r_0^4 + \frac{2}{3}B^2 \ln r_0 - \frac{1}{3}B^2\right) + \mathcal{O}(B^4). \tag{2.26}$$

where we used $\beta' = \beta\sqrt{f} = \beta$ at the boundary $r_\Lambda \to \infty$.

Therefore, $\Delta S_{\rm E}$ (which is the difference between the AdS$_5$ black hole (2.20) and thermal-AdS$_5$ (2.26) on-shell Euclidean actions) becomes

$$\Delta S_{\rm E} = S_{\rm bh} - S_{\rm thermal} = -\beta\left(r_h^4 - r_0^4 - \frac{1}{2}M + \frac{2}{3}B^2 \ln\left(\frac{r_h}{r_0}\right)\right) + \mathcal{O}(B^4)\ . \tag{2.27}$$

JHEP05(2015)121

2.2.3 AdS$_5$-soliton

Since, black hole (2.11) and AdS$_5$-soliton (2.14) are equivalent Euclidean geometries, their on-shell Euclidean actions take similar form. In fact, the on-shell Euclidean action of AdS$_5$-soliton can be found by merely replacing r_h by r_0 in the on-shell Euclidean action for the black hole [35]. Therefore, the difference between the on-shell actions $S_{\rm bh}$ of the black hole (2.20) and $S_{\rm soliton}$ of AdS$_5$-soliton geometries is simply

$$\Delta S_{\rm E} = S_{\rm bh} - S_{\rm soliton} = -\beta \left(r_h^4 - r_0^4 + \frac{2}{3} B^2 \ln \frac{r_h}{r_0} \right) + \mathcal{O}(B^4) \ . \tag{2.28}$$

3 Confinement-deconfinement phase transition in holographic models of QCD for $B \ll T^2$

In this section, we compute the critical temperature T_c of the confinement-deconfinement phase transition in hard-wall AdS/QCD, and holographic duals of flavored and unflavored $\mathcal{N} = 4$ SYM on $\mathbb{R}^3 \times \mathrm{S}^1$.

3.1 Confinement-deconfinement phase transition in hard-wall AdS/QCD

For hard-wall AdS/QCD [36],[3] we determine the critical temperature $T_c(B)$ of the confinement-deconfinement phase transition by first determining the critical radius of the horizon $r_h = r_{hc}$ from the condition that the difference between the Euclidean actions for the black hole and thermal-AdS$_5$ solutions vanish at $r_h = r_{hc}$, i.e., $\Delta S_{\rm E}(r_h = r_{hc}) = 0$. For $B \ll T^2$, requiring $\Delta S_{\rm E}(r_{hc}) = 0$ in (2.27), we find the constraint equation for the critical radius of the horizon r_{hc} to be

$$r_{hc}^4 + \frac{2}{3} B^2 \ln \left(\frac{r_{hc}}{r_0} \right) - 2 r_0^4 + \mathcal{O}(B^4) = 0, \tag{3.1}$$

which can be solved numerically for $r_{hc}(B, r_0)$. Note that, we have fixed $M = 2r_0^4$ in (2.27), so that (3.1) reduces to the constraint equation found in [48, 49] at $B = 0$, which is $r_{hc}^4 = 2r_0^4$. Once we find the solution for r_{hc} from the constraint equation (3.1), we can use (2.12) to find $T_c = T(r_h = r_{hc}, M = 2r_0^4)$. The plot of the numerical solution for $T_c(B, r_0)$ for $B \ll T^2$ is given in figure 1, and the numerical plot clearly shows that $T_c(B)$ decreases with increasing $B \ll T^2$ in agreement with the *inverse magnetic catalysis* recently found in lattice QCD for $B \lesssim 1\,\mathrm{GeV}^2$ [19].

3.2 Confinement-deconfinement phase transition in holographic dual of unflavored $\mathcal{N} = 4$ SYM on $\mathbb{R}^3 \times \mathrm{S}^1$

For the holographic dual of unflavored $\mathcal{N} = 4$ SYM on $\mathbb{R}^3 \times \mathrm{S}^1$,[4] we study the confinement-deconfinement phase transition by using the same Einstein-Maxwell action in $5D$ as we used

[3] For the hard-wall AdS/QCD model, the bulk magnetic field $B = F_{xy}(x, r)$ and the corresponding bulk gauge potential $A_\mu(x, r) = \frac{1}{2} B(x\delta^y_\mu - y\delta^x_\mu)$ are dual to the boundary magnetic field $B = F_{xy}(x, r = \infty)$ and the corresponding boundary gauge potential $A_\mu(x) = A_\mu(x, r = \infty)$ of the U(1)$_V$ subgroup of the SU(N_f) global flavor group of QCD. And, the boundary vector gauge potential $A_\mu(x)$ couples to the boundary conserved vector current $J^\mu_V(x)$.

[4] For the unflavored $\mathcal{N} = 4$ SYM case, the bulk magnetic field $B = F_{xy}(x, r)$ and the corresponding bulk gauge potential $A_\mu(x, r) = \frac{1}{2} B(x\delta^y_\mu - y\delta^x_\mu)$ are dual to the boundary magnetic field $B = F_{xy}(x, r = \infty)$

JHEP05(2015)121

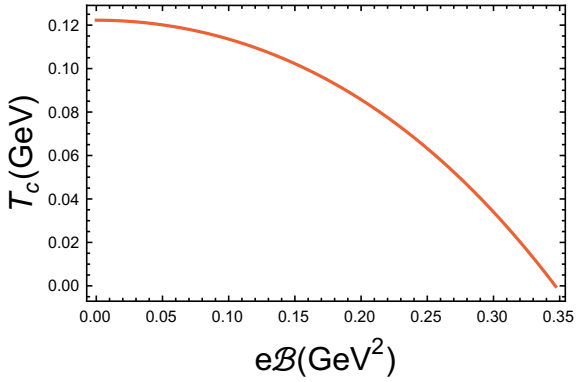

Figure 1. Critical temperature $T_c(B)$ of the hard-wall AdS/QCD with $r_0 = \frac{m_\rho}{2.405} = 0.323\,\text{GeV}$ [48]. Note: $\mathcal{B} = \sqrt{3}B$ is the physical magnetic field at the boundary [50].

for the hard-wall AdS/QCD, and the analysis will be similar to the hard-wall AdS/QCD case but, for the unflavored $\mathcal{N} = 4$ SYM on $\mathbb{R}^3 \times \text{S}^1$ case, we compactify the black hole solution in the z direction into a circle of length l, and compare its free energy with the free energy of AdS_5-soliton solution (2.14) instead of the thermal-AdS_5 solution (2.13) that we used for the hard-wall AdS/QCD.

It is easy to see from (2.28) that the critical radius of the horizon $r_h = r_{hc}$ at which $\Delta S_{\text{E}}(r_h = r_{hc}) = 0$ is given by $r_h = r_{hc} = r_0$. Therefore, using (2.12), the critical temperature $T_c = T(r_h = r_{hc} = r_0)$ becomes,

$$T_c = \frac{r_0}{2\pi}\left(1 + \frac{M}{r_0^4} - \frac{2}{3}B^2\left(\frac{1}{2r_0^4} - \frac{\ln r_0}{r_0^4}\right)\right) + \mathcal{O}(B^4) = \frac{1}{l}\ . \tag{3.2}$$

Fixing $M = r_0^4$ so that we reproduce the correct $B = 0$ result $T_c(B = 0) = \frac{r_0}{\pi}$, and fixing r_0 from the value of T_c at $B = 0$, which we denote as T_c^0, we can write (3.2) in terms of $T_c^0 = \frac{r_0}{\pi}$ as

$$T_c = T_c^0\left(1 - \left(\frac{B}{B_c}\right)^2\right) + \mathcal{O}(B^4) \tag{3.3}$$

where we defined the critical magnetic field $B_c = \frac{\sqrt{6}\pi^2(T_c^0)^2}{1-2\ln(LT_c^0\pi)}$ and L is the radius of the AdS spacetime. From (3.3), it is easy to see that T_c is a decreasing function with increasing $B \ll T^2$ in qualitative agreement with the recent lattice QCD result [19].

3.3 Confinement-deconfinement phase transition in holographic dual of flavored $\mathcal{N} = 4$ SYM on $\mathbb{R}^3 \times \text{S}^1$

In the previous subsection, we have studied the confinement-deconfinement phase transition in the holographic dual of unflavored $\mathcal{N} = 4$ SYM on $\mathbb{R}^3 \times \text{S}^1$ using the backreacted black hole and AdS_5-soliton geometries, from which, we can infer a simple prescription of finding T_c in any backreacted black hole and AdS_5-soliton based models.

and the boundary gauge potential $A_\mu(x) = A_\mu(x, r = \infty)$ of the U(1) subgroup of the $\text{SU}(4)_R$ global R-symmetry group of $\mathcal{N} = 4$ SYM which couples to the boundary R-current J_R^μ.

JHEP05(2015)121

The prescription is, first find the backreacted metric and the Hawking temperature $T(r_h)$ of the black hole, then the critical temperature T_c is simply given by $T_c = T(r_h = r_0)$ where r_0 can be fixed by the value of $T_c^0 = T_c(B = 0)$.

Therefore, using this prescription, we can determine $T_c(N_f, B)$ of the holographic dual of flavored $\mathcal{N} = 4$ SYM on $\mathbb{R}^3 \times \mathrm{S}^1$. To this end we will use the backreacted metric of D3/D7 model given in [38] where the authors have also found the Hawking temperature $T(\frac{N_f}{N_c}, B)$ including the backreaction of N_f $D7$-branes and magnetic field B[5] to be, see eq. 3.1 of [38],[6]

$$T = \frac{r_h}{\pi}\left(1 + \frac{\lambda_h}{64\pi^2}\frac{N_f}{N_c}\left(1 - 2\sqrt{1 + \frac{B^2}{r_h^4}}\right)\right) + \mathcal{O}((N_f/N_c)^2). \tag{3.4}$$

Since the on-shell Euclidean action of the black hole solution (including the backreaction of N_f $D7$-branes and magnetic field B) has also been given in eq. 3.14 of [38], in order to find the corresponding Euclidean action of the AdS_5-soliton, all we need to do is replace r_h by r_0 in eq. 3.14 of [38]. Hence, the difference between the two on-shell Euclidean actions vanishes at the critical radius of the horizon $r_h = r_{hc} = r_0$. And, using $r_h = r_{hc} = r_0$ in (3.4), the critical temperature $T_c = T(r_h = r_{hc} = r_0)$ of the confinement-deconfinement phase transition in flavored $\mathcal{N} = 4$ SYM on $\mathbb{R}^3 \times \mathrm{S}^1$ becomes

$$T_c = \frac{r_0}{\pi}\left(1 + \frac{\lambda_h}{64\pi^2}\frac{N_f}{N_c}\left(1 - 2\sqrt{1 + \frac{B^2}{r_0^4}}\right)\right) + \mathcal{O}((N_f/N_c)^2), \tag{3.5}$$

which can be written in terms of $T_c^0 = T_c(N_f = 0, B = 0) = \frac{r_0}{\pi}$ as

$$T_c = T_c^0\left(1 + \frac{\lambda_h}{64\pi^2}\frac{N_f}{N_c}\left(1 - 2\sqrt{1 + \frac{1}{\pi^4}\frac{B^2}{(T_c^0)^4}}\right)\right) + \mathcal{O}((N_f/N_c)^2), \tag{3.6}$$

where λ_h is the value of the 't Hooft coupling fixed at the horizon r_h, that is, $\lambda_h = 4\pi g_s e^{\phi_h} N_c$ where g_s is the string coupling constant and $\phi(r)$ is the dilaton scalar field.

Note that, for $B = 0$, (3.6) reduces to

$$T_c = T_c^0\left(1 - \frac{\lambda_h}{64\pi^2}\frac{N_f}{N_c}\right) + \mathcal{O}((N_f/N_c)^2), \tag{3.7}$$

which is in a qualitative agreement with the hard-wall AdS/QCD [51], functional renormalization group study of QCD [52], and lattice QCD [53] results which show that T_c decreases with increasing number of flavors N_f at zero magnetic field $B = 0$ and chemical potential $\mu = 0$.

[5]For the $D3/D7$ model, we use a bulk magnetic field which corresponds to the Kalb-Ramond two form field $B_{xy}(x, r)$. And, also note that for the DBI action of the probe $D7$ brane, the gauge invariant and physically significant field strength is given by $\mathcal{F}_{mn} = F_{mn} + B_{mn} = \partial_m \mathcal{A}_n(x) - \partial_n \mathcal{A}_m(x)$ which is the sum of Maxwell's field strength F_{mn} and the Kalb-Ramond two form field B_{mn}. And, the bulk magnetic field $B_{xy}(x, r)$ and the corresponding bulk gauge potential $\mathcal{A}_\mu(x, r)$ are dual to the boundary magnetic field $B = B_{xy}(x, r = \infty)$ and the boundary gauge potential $\mathcal{A}_\mu(x) = \mathcal{A}_\mu(x, r = \infty)$ of the $\mathrm{U}(1)_V$ subgroup of the $\mathrm{SU}(N_f)$ global flavor group of the $\mathcal{N} = 2$ supersymmetric field theory which couples to the boundary vector current $\mathcal{J}_V^\mu(x)$, see, for example, ref. [37]. For our case, $F_{mn} = 0$ but $B_{mn} = B_{xy}$.

[6]In eq. 3.1 of [38], T is written in terms of r_m^4 and ϵ_h. Here, we have used eq. 2.35 and 3.4 of [38] (which relates $\epsilon_h = \frac{\lambda_h}{8\pi^2}\frac{N_f}{N_c}$ and $r_m^2 = B$, respectively) in order to write T explicitly in terms of λ_h, $\frac{N_f}{N_c}$, and B.

JHEP05(2015)121

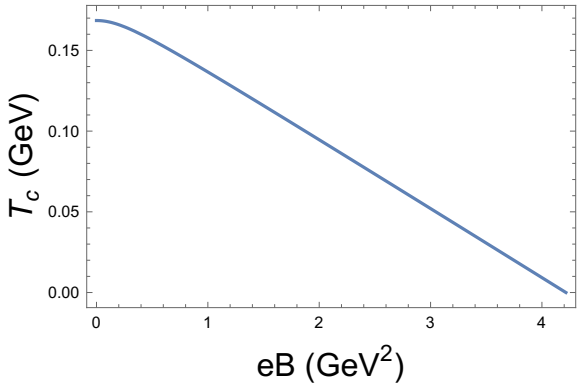

Figure 2. Critical temperature $T_c(B)$ of flavored $\mathcal{N} = 4$ SYM on $R^3 \times S^1$ (3.6) using $T_c^0 = 0.175\,\text{GeV}$ and $\lambda_h = 23 \times \frac{N_c}{N_f}$.

We have plotted (3.6) in figure 2 which clearly shows that $T_c(B)$ decreases with increasing $B \ll T^2$ in agreement with the *inverse magnetic catalysis* recently found in lattice QCD for $B \lesssim 1\,\text{GeV}^2$ [19].

4 Conclusion

The observation of *inverse magnetic catalysis*, for $B \lesssim 1\,\text{GeV}^2$, in the recent study of QCD on the lattice [19], instead of *magnetic catalysis* as predicted by most models of QCD [1–16], has posed a serious challenge both for the holographic and non-holographic models of QCD. Therefore, motivated by gaining new insight into this problem, we have studied the $T - B$ phase diagrams of hard-wall AdS/QCD, and holographic duals of flavored and unflavored $\mathcal{N}$=4 SYM on $\mathbb{R}^3 \times \text{S}^1$ for $B \ll T^2$.

We have found that the $T-B$ phase diagrams of hard-wall AdS/QCD, and holographic duals of flavored and unflavored $\mathcal{N}$=4 SYM on $\mathbb{R}^3 \times \text{S}^1$ (which are based on the study of the confinement-deconfinement phase transition) are consistent with the recent lattice QCD result [19] but opposite to the results of the other holographic models of QCD (which are based on the study of the chiral-symmetry breaking phase transition) [11–16]. As it can be seen in figure 1, figure 2, and eq. (3.3), we have found that the critical temperature $T_c(B)$ decreases with increasing $B \ll T^2$ in agreement with the *inverse magnetic catalysis* observed in the recent lattice QCD result for $B \lesssim 1\,\text{GeV}^2$ [19].

However, we would like to emphasize the fact that the vanishing of $T_c(B)$, at some critical magnetic field B_c, as it can be seen in figure 1, figure 2, and eq. (3.3), might be the artifact of our usage of the backreacted black hole solution only for small magnetic field $B \ll T^2$ and $N_f \ll N_c$ limits. Had we used the exact solution for the backreacted black hole solution, for any value of B and N_f, the critical temperature $T_c(B)$ might not necessarily vanish at some critical magnetic field B_c.

For example, in the large magnetic field $B \gg T^2$ limit, the Hawking temperature of the black hole geometry of [50] is given by $T(B \gg T^2) = \frac{3}{2}\frac{r_h}{\pi}$ (A.3), which according to the prescription of finding the critical temperature T_c given in subsection 3.3, the critical

JHEP05(2015)121

temperature T_c of the unflavored $\mathcal{N}=4$ SYM on $\mathbb{R}^3 \times \mathrm{S}^1$ for large magnetic field $B \gg T^2$ will be $T_c(B \gg T^2) = \frac{3}{2}\frac{r_0}{\pi} = \frac{3}{2}T_c(B=0)$, which means that $T_c(B \gg T^2) > T_c(B = 0)$. Therefore, $T_c(B)$, of unflavored $\mathcal{N}=4$ SYM on $\mathbb{R}^3 \times \mathrm{S}^1$, is not a monotonically decreasing function of B, and it will eventually start to increase for large magnetic field B and asymptotes to the constant value $T_c(B \gg T^2) = \frac{3}{2}T_c(B=0)$.

Similarly, for hard-wall AdS/QCD, the critical temperature $T_c(B \gg T^2) = \frac{3}{\sqrt{2}}\frac{r_0}{\pi}$ (A.16), but from (3.1), one can see that $T_c(B=0) = 2^{1/4}\frac{r_0}{\pi}$, see also [48, 49], which means that $T_c(B \gg T^2) > T_c(B=0)$. Therefore, $T_c(B)$ of hard-wall AdS/QCD, is not a monotonically decreasing function of B, and it will eventually start to increase for large magnetic field B and asymptotes to the constant value $T_c(B \gg T^2) = \frac{3}{\sqrt{2}}\frac{r_0}{\pi}$. We leave the holographic computation of $T_c(B)$ for arbitrary value of B for future investigations.

This eventual increasing (after initially decreasing for small B) of $T_c(B)$ for large B has also been predicted in some very recent non-holographic studies of the chiral-symmetry breaking phase transition in QCD [54, 55], and it has been related to the asymptotic freedom and dimensional reduction of QCD at large magnetic field B.

The *inverse magnetic catalysis* we found in this paper, from our study of the confinement-deconfinement phase transition in the holographic models of QCD (hard-wall AdS/QCD, and holographic duals of flavored and unflavored $\mathcal{N}$=4 SYM on $\mathbb{R}^3 \times \mathrm{S}^1$), is also qualitatively similar to the inverse magnetic catalysis observed in the non-holographic studies of the confinement-deconfinement phase transition in QCD, such as, MIT bag model [56], chiral perturbation theory with two quark flavors [57], and QCD at large-N_c [58].

Acknowledgments

The author thanks Ho-Ung Yee for stimulating discussions, critical reading of the draft, and giving me important feedbacks which greatly improved the clarity of the draft. The author also thanks Bo Ling, and Misha Stephanov for very helpful discussions.

A Confinement-deconfinement phase transition in hard-wall AdS/QCD for $B \gg T^2$

In this appendix, we compute the critical temperature $T_c(B)$ of the confinement-deconfinement phase transition in hard-wall AdS/QCD for large magnetic field $B \gg T^2$.

For $B \gg T^2$, the black hole solution is $\mathrm{AdS}_3 \times T^2$ black hole or $BTZ \times T^2$ [50]

$$ds^2_{\rm bh} = 3r^2\left(-f(r)dt^2 + dz^2\right) + \frac{B}{\sqrt{3}}\left(dx^2+dy^2\right) + \frac{dr^2}{3f(r)r^2}\,, \tag{A.1}$$

$$f(r) = 1 - \frac{M}{r^2}\,. \tag{A.2}$$

and, the Hawking temperature T becomes

$$T = \frac{1}{\beta} = U'(r_h) = \frac{3}{2}\frac{r_h}{\pi}\,, \tag{A.3}$$

where $M = r_h^2$ is the mass of the black hole, $U(r) = r^2 f(r)$, the radius of the horizon r_h is defined by requiring $f(r = r_h) = 0$, and β is the length of the thermal circle.

Note that the transverse $x - y$ plane to the direction of the magnetic field $B = B_z$ of the black hole solution (A.1) is compactified to a 2-torus T^2 [50] which is similar to the dimensional reduction that appears in field theories in an external magnetic field B.

For $B \gg \Lambda_{IR}^2 \sim r_0^2$, the thermal-AdS$_3 \times T^2$ solution can be found from the black hole solution by setting the mass of the black hole M to zero, that is,

$$ds^2_{\text{thermal}} = 3r^2\left(-dt^2 + dz^2\right) + \frac{B}{\sqrt{3}}\left(dx^2 + dy^2\right) + \frac{dr^2}{3r^2}\,. \tag{A.4}$$

The on-shell Euclidean action $S_{\text{E}} = S_{\text{bh}}$ (2.8) for the black hole solution with $B \gg T^2$ (A.1) is

$$S_{\text{bh}} = S_{\text{bulk}} + S_{\text{bndy}}, \tag{A.5}$$

where the on-shell Euclidean bulk action S_{bulk} of the black hole solution for $B \gg T^2$ is

$$S_{\text{bulk}} = \int_0^\beta dt_E \int_{r_h}^{r_\Lambda} dr\sqrt{g}\left(4 + \frac{2}{3}B^2 g^{xx} g^{yy}\right), \tag{A.6}$$

$$= 6\int_0^\beta dt_E \int_{r_h}^{r_\Lambda} dr\sqrt{g}\,, \tag{A.7}$$

and, it turned out, we will not need the on-shell Euclidean boundary action of the black hole to remove the UV divergences, so we set $S_{\text{bndy}} = 0$ for $B \gg T^2$. Hence, the on-shell Euclidean action of the black hole S_{bh} (A.5) becomes

$$S_{\text{bh}} = S_{\text{bulk}} + S_{\text{bndy}} = 6\int_0^\beta dt_E \int_{r_h}^{r_\Lambda} dr\sqrt{g}\,, \tag{A.8}$$

which (after using the black hole metric for $B \gg T^2$ (A.1), evaluating the integrals, and simplifying) gives

$$S_{\text{bh}} = 3\beta B\left(r_\Lambda^2 - r_h^2\right). \tag{A.9}$$

The on-shell Euclidean action $S_{\text{E}} = S_{\text{thermal}}$ (2.8) for the thermal-AdS solution with $B \gg \Lambda_{IR}^2 \sim r_0^2$ (A.4) is

$$S_{\text{thermal}} = S_{\text{tbulk}} + S_{\text{tbndy}}, \tag{A.10}$$

where the on-shell Euclidean bulk action S_{tbulk} of the thermal-AdS for $B \gg \Lambda_{IR}^2 \sim r_0^2$ is

$$S_{\text{tbulk}} = \int_0^{\beta'} dt_E \int_{r_0}^{r_\Lambda} dr\sqrt{g}\left(4 + \frac{2}{3}B^2 g^{xx} g^{yy}\right), \tag{A.11}$$

and, it turned out, we will not need the on-shell Euclidean boundary action S_{tbndy} of the thermal-AdS for $B \gg \Lambda_{IR}^2 \sim r_0^2$ to remove the UV divergences, so we set $S_{\text{tbndy}} = 0$ for $B \gg \Lambda_{IR}^2 \sim r_0^2$.

The thermal-AdS bulk action S_{tbulk} (A.11) (after using the thermal-AdS metric for $B \gg \Lambda_{IR}^2 \sim r_0^2$ (A.4), evaluating the integrals, simplifying, and using $\beta' = \beta\sqrt{f} = \beta(1 -$

JHEP05(2015)121

$\frac{1}{2}\frac{r_h^2}{r_\Lambda^2}$) near the boundary) becomes

$$\begin{aligned} S_{\text{tbulk}} &= 3\beta\sqrt{f}B(r_\Lambda^2 - r_0^2) \\ &= 3\beta B\left(r_\Lambda^2 - \frac{1}{2}r_h^2 - r_0^2\right). \end{aligned} \tag{A.12}$$

Hence,

$$S_{\text{thermal}} = S_{\text{tbulk}} = 3\beta B\left(r_\Lambda^2 - \frac{1}{2}r_h^2 - r_0^2\right). \tag{A.13}$$

Therefore, ΔS_{E} (which is the difference between the black hole (A.9) and thermal-AdS_5 (A.13) on-shell Euclidean actions) becomes

$$\begin{aligned} \Delta S_{\text{E}} &= S_{\text{bh}} - S_{\text{thermal}} \\ &= 3\beta B\left(r_0^2 - \frac{r_h^2}{2}\right) \\ &= 3\beta B\left(r_0^2 - \frac{2}{9}\pi^2 T^2\right), \end{aligned} \tag{A.14}$$

for $B \gg T^2$.

For $B \gg T^2$, requiring $\Delta S_{\text{E}}(T_c) = 0$ (A.14), we find the constraint equation for the critical temperature T_c to be

$$r_0^2 - \frac{2}{9}\pi^2 T_c^2 = 0, \tag{A.15}$$

which can be solved for T_c to give

$$T_c(B, r_0) = \frac{3}{\sqrt{2}}\frac{r_0}{\pi}. \tag{A.16}$$

References

[1] V.P. Gusynin, V.A. Miransky and I.A. Shovkovy, *Catalysis of dynamical flavor symmetry breaking by a magnetic field in* $(2+1)$*-dimensions*, *Phys. Rev. Lett.* **73** (1994) 3499 [*Erratum ibid.* **76** (1996) 1005] [hep-ph/9405262] [INSPIRE].

[2] V.A. Miransky and I.A. Shovkovy, *Magnetic catalysis and anisotropic confinement in QCD*, *Phys. Rev.* **D 66** (2002) 045006 [hep-ph/0205348] [INSPIRE].

[3] A.J. Mizher, M.N. Chernodub and E.S. Fraga, *Phase diagram of hot QCD in an external magnetic field: possible splitting of deconfinement and chiral transitions*, *Phys. Rev.* **D 82** (2010) 105016 [arXiv:1004.2712] [INSPIRE].

[4] E.S. Fraga and A.J. Mizher, *Can a strong magnetic background modify the nature of the chiral transition in QCD?*, *Nucl. Phys.* **A 820** (2009) 103C [arXiv:0810.3693] [INSPIRE].

[5] R. Gatto and M. Ruggieri, *Deconfinement and chiral symmetry restoration in a strong magnetic background*, *Phys. Rev.* **D 83** (2011) 034016 [arXiv:1012.1291] [INSPIRE].

JHEP05(2015)121

[6] R. Gatto and M. Ruggieri, *Dressed Polyakov loop and phase diagram of hot quark matter under magnetic field*, *Phys. Rev.* **D 82** (2010) 054027 [arXiv:1007.0790] [INSPIRE].

[7] A.A. Osipov, B. Hiller, A.H. Blin and J. da Providencia, *Dynamical chiral symmetry breaking by a magnetic field and multi-quark interactions*, *Phys. Lett.* **B 650** (2007) 262 [hep-ph/0701090] [INSPIRE].

[8] K. Kashiwa, *Entanglement between chiral and deconfinement transitions under strong uniform magnetic background field*, *Phys. Rev.* **D 83** (2011) 117901 [arXiv:1104.5167] [INSPIRE].

[9] K.G. Klimenko, *Three-dimensional Gross-Neveu model at nonzero temperature and in an external magnetic field*, *Theor. Math. Phys.* **90** (1992) 1 [*Teor. Mat. Fiz.* **90** (1992) 3] [INSPIRE].

[10] J. Alexandre, K. Farakos and G. Koutsoumbas, *Magnetic catalysis in QED_3 at finite temperature: beyond the constant mass approximation*, *Phys. Rev.* **D 63** (2001) 065015 [hep-th/0010211] [INSPIRE].

[11] V.G. Filev, C.V. Johnson, R.C. Rashkov and K.S. Viswanathan, *Flavoured large-N gauge theory in an external magnetic field*, *JHEP* **10** (2007) 019 [hep-th/0701001] [INSPIRE].

[12] T. Albash, V.G. Filev, C.V. Johnson and A. Kundu, *Finite temperature large-N gauge theory with quarks in an external magnetic field*, *JHEP* **07** (2008) 080 [arXiv:0709.1547] [INSPIRE].

[13] C.V. Johnson and A. Kundu, *External fields and chiral symmetry breaking in the Sakai-Sugimoto model*, *JHEP* **12** (2008) 053 [arXiv:0803.0038] [INSPIRE].

[14] O. Bergman, G. Lifschytz and M. Lippert, *Response of holographic QCD to electric and magnetic fields*, *JHEP* **05** (2008) 007 [arXiv:0802.3720] [INSPIRE].

[15] N. Evans, T. Kalaydzhyan, K.-Y. Kim and I. Kirsch, *Non-equilibrium physics at a holographic chiral phase transition*, *JHEP* **01** (2011) 050 [arXiv:1011.2519] [INSPIRE].

[16] M.S. Alam, V.S. Kaplunovsky and A. Kundu, *Chiral symmetry breaking and external fields in the Kuperstein-Sonnenschein model*, *JHEP* **04** (2012) 111 [arXiv:1202.3488] [INSPIRE].

[17] F. Preis, A. Rebhan and A. Schmitt, *Inverse magnetic catalysis in dense holographic matter*, *JHEP* **03** (2011) 033 [arXiv:1012.4785] [INSPIRE].

[18] A. Ballon-Bayona, *Holographic deconfinement transition in the presence of a magnetic field*, *JHEP* **11** (2013) 168 [arXiv:1307.6498] [INSPIRE].

[19] G.S. Bali et al., *The QCD phase diagram for external magnetic fields*, *JHEP* **02** (2012) 044 [arXiv:1111.4956] [INSPIRE].

[20] D.E. Kharzeev, K. Landsteiner, A. Schmitt and H.-U. Yee, *'Strongly interacting matter in magnetic fields': an overview*, *Lect. Notes Phys.* **871** (2013) 1 [arXiv:1211.6245] [INSPIRE].

[21] V. Skokov, A.Y. Illarionov and V. Toneev, *Estimate of the magnetic field strength in heavy-ion collisions*, *Int. J. Mod. Phys.* **A 24** (2009) 5925 [arXiv:0907.1396] [INSPIRE].

[22] D.E. Kharzeev, L.D. McLerran and H.J. Warringa, *The effects of topological charge change in heavy ion collisions: 'event by event P and CP-violation'*, *Nucl. Phys.* **A 803** (2008) 227 [arXiv:0711.0950] [INSPIRE].

[23] K. Fukushima, D.E. Kharzeev and H.J. Warringa, *The chiral magnetic effect*, *Phys. Rev.* **D 78** (2008) 074033 [arXiv:0808.3382] [INSPIRE].

JHEP05(2015)121

[24] D. Kharzeev, *Parity violation in hot QCD: why it can happen and how to look for it*, *Phys. Lett.* **B 633** (2006) 260 [hep-ph/0406125] [INSPIRE].

[25] STAR collaboration, S.A. Voloshin, *Probe for the strong parity violation effects at RHIC with three particle correlations*, *Indian J. Phys.* **85** (2011) 1103 [arXiv:0806.0029] [INSPIRE].

[26] STAR collaboration, B.I. Abelev et al., *Azimuthal charged-particle correlations and possible local strong parity violation*, *Phys. Rev. Lett.* **103** (2009) 251601 [arXiv:0909.1739] [INSPIRE].

[27] ALICE collaboration, I. Selyuzhenkov, *Anisotropic flow and other collective phenomena measured in Pb-Pb collisions with ALICE at the LHC*, *Prog. Theor. Phys. Suppl.* **193** (2012) 153 [arXiv:1111.1875] [INSPIRE].

[28] T. Vachaspati, *Magnetic fields from cosmological phase transitions*, *Phys. Lett.* **B 265** (1991) 258 [INSPIRE].

[29] R.C. Duncan and C. Thompson, *Formation of very strongly magnetized neutron stars — implications for gamma-ray bursts*, *Astrophys. J.* **392** (1992) L9 [INSPIRE].

[30] E. Witten, *Anti-de Sitter space, thermal phase transition and confinement in gauge theories*, *Adv. Theor. Math. Phys.* **2** (1998) 505 [hep-th/9803131] [INSPIRE].

[31] J. Sonnenschein, *Stringy confining Wilson loops*, PoS(tmr2000)008 [hep-th/0009146] [INSPIRE].

[32] G.T. Horowitz and R.C. Myers, *The AdS/CFT correspondence and a new positive energy conjecture for general relativity*, *Phys. Rev.* **D 59** (1998) 026005 [hep-th/9808079] [INSPIRE].

[33] S. Surya, K. Schleich and D.M. Witt, *Phase transitions for flat AdS black holes*, *Phys. Rev. Lett.* **86** (2001) 5231 [hep-th/0101134] [INSPIRE].

[34] J. Casalderrey-Solana, H. Liu, D. Mateos, K. Rajagopal and U.A. Wiedemann, *Gauge/string duality, hot QCD and heavy ion collisions*, arXiv:1101.0618 [INSPIRE].

[35] M. Natsuume, *AdS/CFT duality user guide*, arXiv:1409.3575 [INSPIRE].

[36] E. D'Hoker and P. Kraus, *Charged magnetic brane solutions in AdS_5 and the fate of the third law of thermodynamics*, *JHEP* **03** (2010) 095 [arXiv:0911.4518] [INSPIRE].

[37] C. Hoyos, T. Nishioka and A. O'Bannon, *A chiral magnetic effect from AdS/CFT with flavor*, *JHEP* **10** (2011) 084 [arXiv:1106.4030] [INSPIRE].

[38] M. Ammon, V.G. Filev, J. Tarrio and D. Zoakos, *$D3/D7$ quark-gluon plasma with magnetically induced anisotropy*, *JHEP* **09** (2012) 039 [arXiv:1207.1047] [INSPIRE].

[39] G. Basar and D.E. Kharzeev, *The Chern-Simons diffusion rate in strongly coupled $N = 4$ SYM plasma in an external magnetic field*, *Phys. Rev.* **D 85** (2012) 086012 [arXiv:1202.2161] [INSPIRE].

[40] K.A. Mamo, *Enhanced thermal photon and dilepton production in strongly coupled $N = 4$ SYM plasma in strong magnetic field*, *JHEP* **08** (2013) 083 [arXiv:1210.7428] [INSPIRE].

[41] G. Arciniega, P. Ortega and L. Patiño, *Brighter branes, enhancement of photon production by strong magnetic fields in the gauge/gravity correspondence*, *JHEP* **04** (2014) 192 [arXiv:1307.1153] [INSPIRE].

[42] R. Critelli, S.I. Finazzo, M. Zaniboni and J. Noronha, *Anisotropic shear viscosity of a strongly coupled non-Abelian plasma from magnetic branes*, *Phys. Rev.* **D 90** (2014) 066006 [arXiv:1406.6019] [INSPIRE].

JHEP05(2015)121

[43] R. Rougemont, R. Critelli and J. Noronha, *Anisotropic heavy quark potential in strongly-coupled $N = 4$ SYM in a magnetic field*, *Phys. Rev.* **D 91** (2015) 066001 [arXiv:1409.0556] [INSPIRE].

[44] J. Erlich, E. Katz, D.T. Son and M.A. Stephanov, *QCD and a holographic model of hadrons*, *Phys. Rev. Lett.* **95** (2005) 261602 [hep-ph/0501128] [INSPIRE].

[45] G.F. de Teramond and S.J. Brodsky, *Hadronic spectrum of a holographic dual of QCD*, *Phys. Rev. Lett.* **94** (2005) 201601 [hep-th/0501022] [INSPIRE].

[46] K. Skenderis, *Lecture notes on holographic renormalization*, *Class. Quant. Grav.* **19** (2002) 5849 [hep-th/0209067] [INSPIRE].

[47] B.-H. Lee, C. Park and S.-J. Sin, *A dual geometry of the hadron in dense matter*, *JHEP* **07** (2009) 087 [arXiv:0905.2800] [INSPIRE].

[48] C.P. Herzog, *A holographic prediction of the deconfinement temperature*, *Phys. Rev. Lett.* **98** (2007) 091601 [hep-th/0608151] [INSPIRE].

[49] C.A. Ballon Bayona, H. Boschi-Filho, N.R.F. Braga and L.A. Pando Zayas, *On a holographic model for confinement/deconfinement*, *Phys. Rev.* **D 77** (2008) 046002 [arXiv:0705.1529] [INSPIRE].

[50] E. D'Hoker and P. Kraus, *Magnetic brane solutions in AdS*, *JHEP* **10** (2009) 088 [arXiv:0908.3875] [INSPIRE].

[51] Y. Kim, B.-H. Lee, S. Nam, C. Park and S.-J. Sin, *Deconfinement phase transition in holographic QCD with matter*, *Phys. Rev.* **D 76** (2007) 086003 [arXiv:0706.2525] [INSPIRE].

[52] J. Braun and H. Gies, *Chiral phase boundary of QCD at finite temperature*, *JHEP* **06** (2006) 024 [hep-ph/0602226] [INSPIRE].

[53] F. Karsch, E. Laermann and A. Peikert, *Quark mass and flavor dependence of the QCD phase transition*, *Nucl. Phys.* **B 605** (2001) 579 [hep-lat/0012023] [INSPIRE].

[54] M. Ferreira, P. Costa, O. Lourenço, T. Frederico and C. Providência, *Inverse magnetic catalysis in the $(2+1)$-flavor Nambu-Jona-Lasinio and Polyakov-Nambu-Jona-Lasinio models*, *Phys. Rev.* **D 89** (2014) 116011 [arXiv:1404.5577] [INSPIRE].

[55] J. Braun, W.A. Mian and S. Rechenberger, *Delayed magnetic catalysis*, arXiv:1412.6025 [INSPIRE].

[56] E.S. Fraga and L.F. Palhares, *Deconfinement in the presence of a strong magnetic background: an exercise within the MIT bag model*, *Phys. Rev.* **D 86** (2012) 016008 [arXiv:1201.5881] [INSPIRE].

[57] N.O. Agasian and S.M. Fedorov, *Quark-hadron phase transition in a magnetic field*, *Phys. Lett.* **B 663** (2008) 445 [arXiv:0803.3156] [INSPIRE].

[58] E.S. Fraga, J. Noronha and L.F. Palhares, *Large-N_c deconfinement transition in the presence of a magnetic field*, *Phys. Rev.* **D 87** (2013) 114014 [arXiv:1207.7094] [INSPIRE].

JHEP05(2015)121